Heliyon 10 (2024) e30677

Contents lists available at ScienceDirect

Heliyon

journal homepage: www.cell.com/heliyon

Research article

Predictive analysis of concrete slump using a stochastic search-consolidated neural network

Yunwen Zhou [a,*], Zhihai Jiang [b], Xizhen Zhu [a]

[a] School of Architecture and Engineering, JiangXi Institute of Applied Science and Technology, Nan Chang, 330000, China
[b] School of Civil Engineering, Nanchang Institute of Technology, Nan Chang, 330000, China

ARTICLE INFO

Keywords:
Sustainable construction
Concrete
Slump
Neural network
Stochastic fractal search

ABSTRACT

Attaining a dependable measurement of concrete slump is crucial as it is a valuable indication of concrete workability. On the other hand, complexities associated with costly traditional approaches have driven engineers to use indirect efficient models such as metaheuristic-based machine learning for approximating the slump. While the literature shows promising application of some metaheuristic techniques for this purpose, the large variety of these algorithms calls for evaluating the most capable ones to keep the solution updated. Stochastic fractal search (SFS) is one of the most powerful optimization algorithms in the literature that has not received appropriate attention in analyzing concrete mechanical parameters. In the present research, a multi-layer perceptron neural network (NN-MLP), is enhanced using the SFS. The proposed SFS-NN-MLP model aims to predict the slump based on the amount of ingredients in the mixture, as well as the curing age of specimens. Accuracy assessment revealed that the proposed model can deal with the assigned task with excellent accuracy. It indicates that the SFS could properly tune the parameters required for training the NN-MLP, and consequently, the trained network could reliably calculate the slump of specimens that were not analyzed before. For comparative validation, the SFS was replaced with two similar optimizers, namely elephant herding optimization algorithm (EHO) and slime mould algorithm (SMA). Based on the calculated mean square errors of 5.6526, 6.1129, and 7.3561 along with mean absolute errors of 4.6657, 5.0078, and 6.3066, as well as the percentage-Pearson correlation coefficients of 78.06 %, 73.95 %, and 58.11 %, respectively for the SFS-NN-MLP, EHO–NN–MLP, and SMA–NN–MLP, it was shown that the SFS-NN-MLP is the most accurate predictor. Hereupon, the SFS-NN-MLP model is recommended to be effectively used for obtaining a cost-efficient approximation of concrete slump in real-world projects.

1. Introduction

Concrete is known as a suitable construction material that has been used in various projects worldwide [1–5]. The prediction of concrete parameters such as compressive strength (CS) is very important and can lead to reducing the time and cost of a project [6]. Scholars stated that the amount of energy consumption and the degree of compatibility with the environment are among two important elements that have to be taken into consideration for designing a mixture in the case of constructing concrete factors [7,8].

* Corresponding author.
E-mail address: zhouyunwen95@163.com (Y. Zhou).

https://doi.org/10.1016/j.heliyon.2024.e30677
Received 18 December 2023; Received in revised form 28 March 2024; Accepted 1 May 2024
Available online 4 May 2024

So far, many numerical/analytical attempts have been made to improve the quality of concrete-based elements. For instance, Bakhshi et al. [9] investigated the design of printable engineered cementitious composite by replacing the cement with different contents; and the specimens were evaluated in terms of setting time and strength. Shakouri Mahmoudabadi et al. [10] studied the response of concrete columns reinforced with glass fiber-reinforced polymer (GFRP) under eccentric loading. Supported by the results of finite element ABAQUS analysis, they observed that the load-carrying capacity falls with the increase of eccentricity. Mozafarjazia and Rabieeb [11]conducted experimental and numerical analyses to evaluate the ductility, load-bearing capacity, and energy absorption of reinforced concrete shear walls. They observed that having a balanced configuration of rebar besides the use of pozzolanic concrete in the wall results in enhancing these three parameters.

In a more general sense, technological advances have facilitated evaluations/measurements in the world of engineering such as sustainable construction projects [12–16]. A more particular example can be structural engineering in which sensitive analyses are performed using computer software to secure a proper design of buildings [17–19]. Likewise, the advent of laboratory utensils and novel modeling approaches have enabled engineers to assess the quality of construction materials [20–24]. However, above these advances, computational intelligence and machine learning (ML) algorithms have facilitated and enhanced the prediction of different engineering variables [25–28]. For instance, Ghasemi and Naser [29] tried to utilize the capability of artificial intelligence for predicting the mechanical properties (i.e., compressive strength) of 3D-printed concrete. There are various machine learning models that have served for modeling the CS of diverse concrete types [30–33]. Previous studies demonstrated the reliable performances of artificial neural networks (ANNs) in dealing with durability, corrosion, and elastic modulus simulation of many different concretes [34–36]. Nguyen et al. [37] utilized the ANN model for prediction tasks and were concerned with the workability parameters of self-compacting concrete and provided appropriate results. Hammoudi et al. [38] proved the applicability of the ANN model for forecasting tasks in compressive strength modeling. In order to evaluate the slump, the CS, and elastic modulus of bentonite plastic concrete, Amlashi et al. [39] also utilized the ANN model together with multivariate adaptive regression splines, and M5 model tree and determined that ANN provided outstanding results compared to other mentioned models. In addition, they have also specified many involved variables that had the largest effect or the least influence on the slump of BPC. Onikeku et al. [40] also evaluated the ANN efficiency as well as multiple linear regression to simulate the compressive strength and slump of different waste materials concrete. Hoang and Pham [41] utilized a traditional ML model called least squares to support vector regression (LS-SVR) and showed that this model can be used in the case of modeling concrete workability.

There are many limitations in the case of experimental-based methods as well as computational optimization by traditional ML algorithms for optimizing concrete mixture proportions [42,43]. Due to the low or average efficiency of traditional methods to deal with highly non-linear and complicated engineering problems, many researchers have focused on the use of metaheuristic methods to optimize previous ML methods. In this optimization, firstly, objective functions are developed and then metaheuristic optimization algorithms are applied in order to perform optimization tasks [44–46]. For instance, Wahab et al. [47] showed the applicability of ANNs trained by particle swarm optimization (PSO), bat algorithm (BA), and grey wolf optimizer (GWO) to model how concrete cylinder strength is influenced by the confinement effect of carbon fiber reinforced polymers. Moayedi et al. [48] utilized ant lion optimization (ALO) to optimize the ANN model for forecasting the concrete slump, and RMSE and mean absolute error (MAE) equal to 3.0286 and 3.7788 were obtained that introduced the ALO as an outstanding optimizer for forecasting aims. Chandwani et al. [49] enhanced the prediction capability of the ANN by using a genetic algorithm. Foong et al. [50] have evaluated the efficiency of three promising approaches teaching-learning-based optimization (TLBO), electromagnetic field optimization (EFO), water cycle algorithm (WCA), and multi-tracker optimization algorithm (MTOA); and found that EFO provided the highest performance. Zhang et al. [51] stated that the traditional single-objective optimization models cannot be perfectly used for multi-objective optimization (MOO) purposes so they suggested an MOO approach considering different ML methods enhanced by metaheuristic algorithms for optimizing concrete mixture proportions. They have demonstrated that the training time for the RF method enhanced by metaheuristic algorithms was about 0.98. Zhang et al. [52] stated that the Pareto front for MOO algorithm is expensive computationally and a MOO model was developed by different ML models optimized by a novel metaheuristic algorithm. They obtained the relationships among different parts and modeled SFC properties on a dataset by utilizing a back propagation neural network (BPNN) model and found that this model provided reliable predictions for UCS with a high correlation coefficient of 0.9663 according to the test set.

Ly et al. [53] optimized Levenberg–Marquardt-based ANN (LMA-ANN) by particle swarm optimization in order to forecast foamed concrete CS (FCCS). LMA-ANN was determined as an accurate and fast predictor. The suggested algorithm was demonstrated as an effective predictor approach in the case of the FCCS with the highest value of R near 0.959. A similar study conducted by Safayenikoo et al. [54] utilized four different wise metaheuristic algorithms including biogeography-based optimization (BBO), moth-flame optimization (MFO), wind-driven optimization (WDO), and salp swarm algorithm (SSA) for optimizing a neural model, called multilayer perceptron (MLP). They stated that the BBO-MLP with RS of 21 showed to have the most accurate model compared to other stated models. Safayenikoo et al. [55] used three different metaheuristic algorithms namely shuffled complex evolution (SCE), the vortex search algorithm (VSA), and multi-verse optimizer (MVO) for enhancing the configuration of multi-layer perceptron (MLP) neural network. Based on the obtained results, they have shown that the prediction error in the case of MLP was considerably reduced around 33 % after using the SCE algorithm.

This study is a continuation of the previous literature for developing novel metaheuristic-based models in slump modeling. For this purpose, an MLP neural network (NN-MLP) is incorporated with stochastic fractal search (SFS) algorithm [56] to create the SFS-NN-MLP hybrid. The literature shows very promising applications of the SFS in optimizing machine learning models with different mechanisms for prediction purposes. For instance, Ye et al. [57] used the SFS to optimize adaptive neuro-fuzzy inference system (ANFIS) applied to the prediction of blast-induced air overpressure. As for ANNs, Moayedi et al. [58] and Nejati et al. [59] proved the competency of this algorithm in tunning weights and biases of ANN for predicting landslide susceptibility and buildings' energy

performance, respectively. From these studies, it can be derived that the SFS has a reliable performance in dealing with intricate and high-dimensional problems. The SFS-NN-MLP in this work analyzes the concrete mixture characteristics and establishes an optimal relationship between them and slump to predict the slump of new specimens. The performance of the suggested model is compared to EHO–NN–MLP (combination of NN-MLP with elephant herding optimization [60]) and SMA–NN–MLP (combination of NN-MLP with slime mould algorithm [61]) which are among the newest similar techniques. Apart from the accuracy comparison of the models, a principal component analysis (PCA) is carried out on the dataset to highlight the importance of concrete mixture ingredients on the slump estimation.

2. Data and modeling methodology

2.1. Data provision

For such studies, the used dataset must provide sufficient information of concrete specimens. Table 1 introduces the characteristics of the used dataset wherein the slump (*cm*) of 103 specimens is measured, along with seven mixture properties including the amount of the used fly ash, superplasticizer, coarse aggregate, water, fine aggregate, and cement (all in kg/m^3). In this work, the mentioned properties are input factors (IF_i, i = 1, 2, …, 7), while slump is the target factor (TF).

As a common process in machine learning works, two sub-datasets are created out of the existing dataset. The information from the bigger dataset is consumed to train the machine learning models, and the information from the smaller dataset is dedicated to testing the prediction reliability. Considering the number of existing data (i.e., 103), the training dataset is composed of information from 82 specimens, and the test dataset is composed of information from the remaining 21 specimens. It can be inferred that 80 % and 20 % of specimens are considered for these datasets, respectively.

Note that, this study uses the dataset in its original format (i.e., without normalization). The reason for this decision is to keep all problem variables fixed to solely focus on the models' performance.

2.2. Methodology

2.2.1. Stochastic fractal search

As one of the most recent search methods, the stochastic fractal search was designed by Salimi [56] in 2015. It is an efficient optimizer that has been successfully used in various fields [63–65]. The optimization using the SFS comprises diffusing and updating major steps. In the first stage, the particles do the exploitation by diffusing around their current position. It can help avoid stuck in local minima. In the second stage, the members' positions are updated regarding the difference between the points in a group [66]. It is also worth noting that, in the diffusion process, the best-fitted agents are involved and consequently, other agents' products are discarded [67].

Based on Markovian stochastic form [56], two well-known statistical methods for generating particles from diffusing task are Levy flight walk and Gaussian walk. The Gaussian walk enables the algorithm to have faster convergence, as well as the ability to detect the global minima [68]. Mathematically, let q_1 and q_2 be random numbers that can vary from 0 to 1, then the Gaussian walk in the diffusion can be written as in Equations (1)–(3).

$$GS_1 = G\left(mn_{Bp}, \delta\right) + \left(q_1\, r_b - q_2\, r_i\right) \tag{1}$$

$$GS_2 = G\left(mn_p, \delta\right) \tag{2}$$

$$\delta = \left|\frac{\log(z)}{z}\left(r_i - r_b\right)\right| \tag{3}$$

where z symbolizes the iteration, and r_b and r_i denote the elite and typical agent, respectively. Also, *G (mn, δ)* gives the Gaussian distribution function with standard deviations and δ mean *mn*.

Table 1
Characteristics of the used dataset.

Provider	Source page	Size	No. of inputs	Inputs	No. of targets	Target
Yeh [62]	http://archive.ics.uci.edu/ml/datasets/Concrete+Slump+Test	103 × 8	7	Slag (IF_1) Fly ash (IF_2) Superplasticizer (IF_3) Coarse aggregate (IF_4) Water (IF_5) Fine aggregate (IF_6) Cement (IF_7)	1	Slump (TF)

Fig. 1(a - h) present the boxplot of the TF and IFs. The values of IF_1, IF_2, IF_3, IF_4, IF_5, IF_6, and IF_7 range in [0.0, 260.0], [0.0, 193.0], [4.4, 19.0], [708.0, 1049.9], [160.0, 240.0], [640.6, 902.0], and [137.0, 374.0] with averages of 149.0, 78.0, 8.5, 884.0, 197.2, 739.6, and 229.9, respectively. Moreover, respective standard deviations are 85.4, 60.5, 2.8, 88.4, 20.2, 63.3, and 78.9. As for the TF, the minimum, average, maximum, and standard deviation value is 0.0, 18.0, 29.0, and 8.7, respectively.

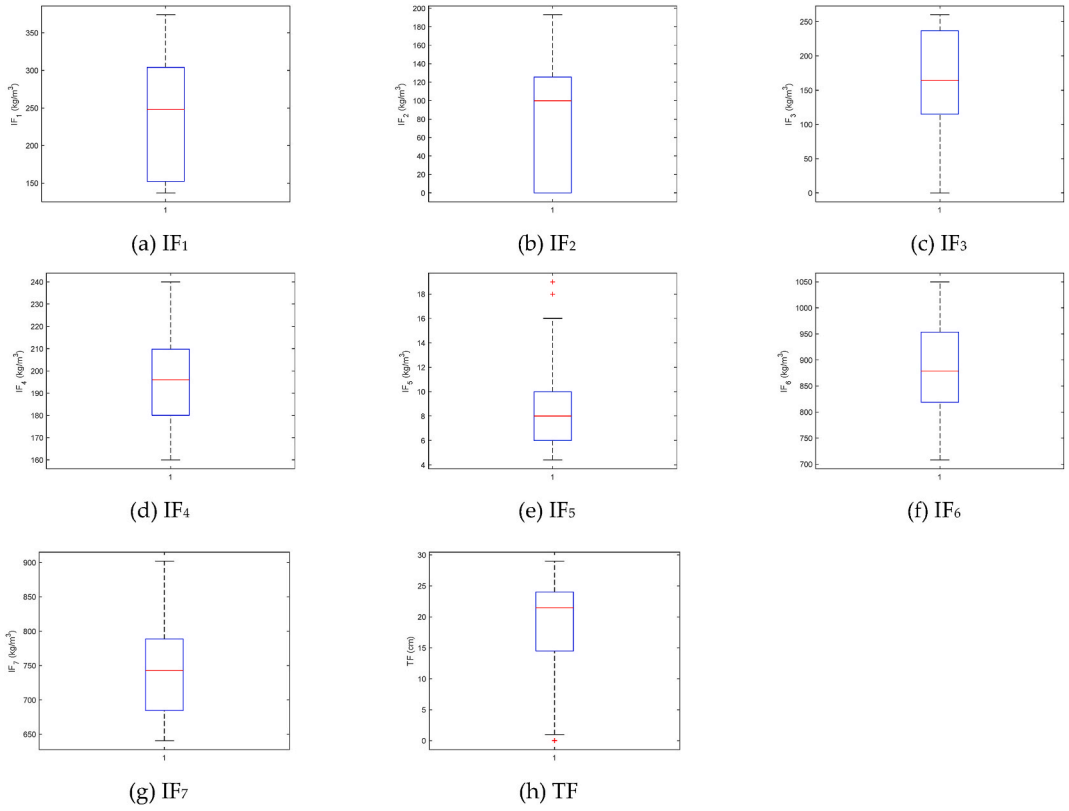

Fig. 1. Boxplot of the TF and IFs.

2.2.2. *Elephant herding optimization*

The EHO is a recently developed hybrid technique used for various optimization aims [60]. As the name denotes, it mimics the complex social behavior of the biggest mammals in the world [69]. Three major assumptions for expressing this behavior are (i) the presence of several groups with a constant number of individuals, (ii) a number of male members of every generation leaving the family to keep living lonely far from the herd, (iii) a matriarch leads whole elephants [60].

The EHO algorithm is based on two major steps, which are described in the following.

a) Clan updating

Let $X_{m,i}$ be the current position of the elephant clan m, then influenced by the corresponding matriarch, this position is updated as in Equation (4).

$$X_{new,m,i} = X_{m,i} + \beta \times \left(X_{best,m} - X_{m,i} \right) \times r \tag{4}$$

where β denotes the scale factor used for setting the impact of the head m on the position. Notably, the assessment of this parameter lies within [0, 1]. Also, $X_{best,m}$ is the fittest member (i.e., the matriarch m) in the clan, and r symbolizes a parameter that could range from 0 to 1. Considering $X_{centre,m}$ as the center of the proposed clan, Equation (5) expresses the update of the fittest individual as it cannot be updated by the mentioned relationship.

$$X_{new,m,i} = \delta \times X_{centre,m} \tag{5}$$

in which δ is the influence of the center on $X_{new,m,i}$ and might range in [0, 1]. Remarkably, the parameter $X_{centre,m}$ for the kth dimension ($1 \leq k < K$) is obtained from Equation (6).

$$X_{centre,m,k} = {}^{1}/_{n_m} \times \sum_{i=1}^{n_m} X_{m,i,k} \tag{6}$$

where n_m defines the number of elephants.

b) 2. Separation

As mentioned previously, it is common in elephant herds that adult male individuals select solitary life instead of being with their family. The separation stage expresses this process as one of the most important steps of the EHO algorithm. To maintain the method in the highest level of robustness, it is supposed that the leaving elephant is the weakest one in each generation. This process is expressed in Equation (7).

$$X_{worst-fitted,m} = X_{min} + (X_{max} - X_{\min} + 1) \times rand \tag{7}$$

in which the lower bound and upper bound of the elephant position are respectively denoted by X_{min} and $X_{\max}$. Besides, the term *rand* represents uniform distribution within [0, 1] [60,70].

2.2.3. Slime mould algorithm

The SMA is inspired by the dynamic behavior of slime mould. This algorithm was suggested by Li, Chen, Wang, Heidari and Mirjalili [61]. During the foraging behavior of an organic matter, the food is sought, surrounded, and digested. The food blocks lie in an interconnected venous network where the SM aims to find the optimal path toward the best one [71]. The algorithm uses an adaptive search strategy for this.

In the first step of the algorithm, the SM uses Equation (8) to approach the food.

$$\overrightarrow{X(t+1)} = \begin{cases} \overrightarrow{X_b(t)} + \overrightarrow{vb} \cdot \left(\overrightarrow{W} \cdot \overrightarrow{X_A(t)} - \overrightarrow{X_B(t)}\right), r < p \\ \overrightarrow{vc} \cdot \overrightarrow{X(t)}, r \geq p \end{cases} \tag{8}$$

where $\overrightarrow{X}$ is the SM's location, $\overrightarrow{X_A}$ and $\overrightarrow{X_B}$ are the location of two randomly selected agents, and $\overrightarrow{X_b}$ is the location of the agent with the best odor concentration discovered so far, $\overrightarrow{W}$ represents the SM weight, $\overrightarrow{vc}$ decreases linearly from 1 to 0, t stands for the current iteration, and $\overrightarrow{vb}$ ranges in $[-a, a]$ where a is calculated by Equation (9).

$$a = \operatorname{arctanh}\left(-\left(\frac{t}{\max_t}\right) + 1\right) \tag{9}$$

Also, p is calculated by Equation (10):

$$p = \tanh|S(i) - DF| \; i \in 1, 2, \ldots, n. \tag{10}$$

where DF stands for the best obtained fitness and $S(i)$ represents the fitness of $\overrightarrow{X}$. Moreover, SM's weight is calculated by Equations (11) and (12).

$$\overrightarrow{W(SmellIndex(i))} = \begin{cases} 1 + r \cdot log\left(\frac{bF - S(i)}{bF - wF} + 1\right), condition \\ 1 - r \cdot log\left(\frac{bF - S(i)}{bF - wF} + 1\right), others \end{cases} \tag{11}$$

$$SmellIndex = sort(S) \tag{12}$$

where r signifies a value randomly selected from 0 to 1, wF and bF stand for the worst and best fitnesses resulted in the present effort, *condition* symbolizes ranking the first half of the swarm based on $S(i)$, and *SmellIndex* shows the ascending order of sorted $S(i)$ s.

The second step simulates wrapping the food. The concentration of the food is affected by three parameters, namely the vein thickness, the flow speed of the cytoplasm, and the potential of the waves released by the bio-oscillator. The SM is tended to the regions with larger food concentrations. Assuming B_U and B_L as the upper and lower bounds, the position is updated as in Equation (13).

$$\overrightarrow{X^*} = \begin{cases} rand \cdot (B_U - B_L) + B_L, rand < z \\ \overrightarrow{X_b(t)} + \overrightarrow{vb} \cdot \left(W \cdot \overrightarrow{X_A(t)} - \overrightarrow{X_B(t)}\right), r < p \\ \overrightarrow{vc} \cdot \overrightarrow{X(t)}, r \geq p \end{cases} \tag{13}$$

where *rand* and r represent a random value in [0, 1].

The next stage is dedicated to capturing the food. As explained, $\overrightarrow{W}$ is the weight which addresses the oscillation frequency of the SM at various food concentrations. It increases the speed of the SM when moving toward potent food sources. Even if the SM reaches a promising food source, some organic members evaluate the remaining regions to determine the best food block.

In the last step, the computational complexity of the algorithm is calculated. Given T as the maximum number of iterations and N as the number of the SM's units in a D-dimensional space, the computational complexity of initialization, fitness evaluation and sorting, weight update, and location update steps can be expressed as $O(N)$, $O(N + N \log N)$, $O(N \times D)$, and $O(N \times D)$, respectively. The general complexity of the algorithm, therefore, is given as $O(N * (1 + T * N * (1 + \log N + 2 * D)))$ [61].

2.2.4. Evaluation criteria

Root mean square error (RMSE) and mean absolute error (MAE), along with percentage-Pearson correlation coefficient (PPCC) are

three criteria that are used for the purpose of accuracy evaluation. These criteria are expressed in Equations (14)–(16).

$$RMSE = \sqrt{\frac{1}{G}\sum_{i=1}^{G}\left[\left(S_{i_{obs}} - S_{i_{pred}}\right)\right]^2} \tag{14}$$

$$MAE = \frac{1}{G}\sum_{I=1}^{G}\left|S_{i_{obs}} - S_{i_{pred}}\right| \tag{15}$$

$$PPCC = \frac{\sum_{i=1}^{G}\left(S_{i_{pred}} - \overline{S_{i_{pred}}}\right)\left(S_{i_{obs}} - \overline{S_{i_{obs}}}\right)}{\sqrt{\sum_{i=1}^{G}\left(S_{i_{pred}} - \overline{S_{i_{pred}}}\right)^2}\sqrt{\sum_{i=1}^{G}\left(S_{i_{obs}} - \overline{S_{i_{obs}}}\right)^2}} \times 100 \tag{16}$$

in which $S_{i\ pred}$ and $S_{i\ obs}$ stand for the forecasted and expected slumps, respectively, for G specimens. Hence, G equals 82 and 21 in the training and testing phases, respectively.

Moreover, a newer index called a20 [72,73] is used for further accuracy comparison. Having *g20* as the number of samples for which $0.8 < S_{i\ obs}/S_{i\ pred} < 1.20$, a20 is expressed in Equation (17) [74]. Note that, it can be calculated only for non-zero $S_{i\ obs}$.

$$a20 = \frac{g20}{G} \tag{17}$$

3. Results and discussion

3.1. Hybrid creation and optimized training

In order to meet the goal of the study, first, the SFS-NN-MLP hybrid must be created. Fig. 2 illustrates the flowchart of creating the model. In this way.

(i) The training data is exposed to the mathematical form of an NN-MLP (7, 7, 1) whose architecture is determined based on the authors' experience and fitness of the data. As shown in Fig. 2, the NN-MLP has 7 input neurons, 7 hidden neurons, and 1 output neuron.
(ii) The equation of the NN-MLP is given to the SFS algorithm for optimizing its weights and biases of NN-MLP [75,76]. In this part, in each iteration of the SFS, the search agents achieve a candidate solution (as per Section 2.2.1) and its quality is quantified using a cost function.
(iii) The SFS iterates 1000 times to present a steady solution. A stopping criterion (i.e., the number of iterations) is checked to continue/eliminate the loop.
(iv) The final solution is saved to create the optimized NN-MLP.

Note that the same process is carried out to develop the EHO–NN–MLP and SMA–NN–MLP hybrids (as per Sections 2.2.2 and 2.2.3).

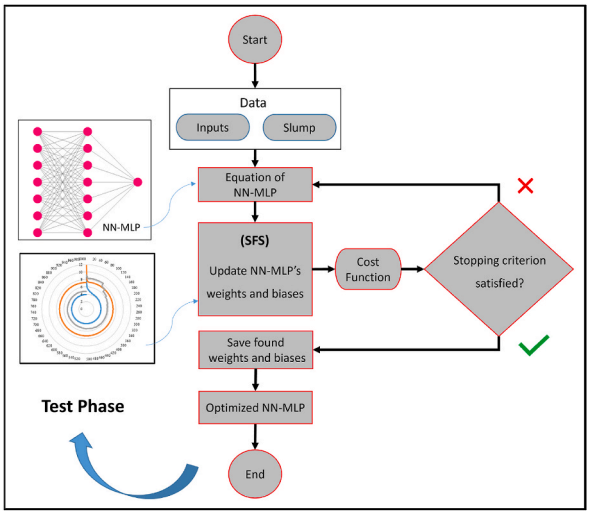

Fig. 2. Flowchart of optimizing NN-MLP using the SFS algorithm.

Further details can be sought in similar previous studies [77–79].

Focusing on the fourth step of this flowchart, Fig. 3 shows how the cost function (i.e., RMSE) converges with the increase of iterations. The cost functions of the SFS-NN-MLP, EHO–NN–MLP, and SMA–NN–MLP start from 8.7090, 11.7443, and 9.2430, and at the end of the 1000th iteration, end up with 3.9336, 4.7621, and 7.1469, respectively. These reductions show the potential of the optimization algorithms in minimizing the error of the NN-MLP model.

3.2. Training quality

When the training of the models is finished, three accuracy criteria are applied to assess the quality. In terms of the RMSE, 3.9336, 4.7621, and 7.1469 are obtained for the SFS-NN-MLP, EHO–NN–MLP, and SMA–NN–MLP, respectively. These error values are associated with the MAEs of 3.1141, 3.6994, and 5.9192. As far as the correlation assessment is concerned, the PPCCs are 89.50 %, 83.92 %, and 58.02 %.

Fig. 4(a–c) show the training results. As is seen, each figure is composed of four sub-figures illustrating (i) a comparison between the forecasted and expected slumps, (ii) the correlation between the forecasted and expected slumps, (iii) the error trend showing the pure difference between the forecasted and expected slumps, and (iv) histogram of these pure error values. According to Fig. 4, while all three techniques have achieved satisfying results, it can be seen that the results of SFS-NN-MLP and EHO–NN–MLP are more promising than SMA–NN–MLP. This inference can be obtained from closer predictions of slump values, higher correlation, lower range of error, and more reasonable histogram of errors.

3.3. Testing quality

While the quality of training reveals learning ability, testing quality shows to what extent the learned knowledge is extrapolatable to external datasets. That's the reason test data is quite different from the train one.

Once the training process ends, the models are applied to test data i.e., 21 specimens. The same accuracy criteria are used for assessing the quality of the test process. Based on the calculated RMSEs of 5.6526, 6.1129, and 7.3561, as well as the MAEs of 4.6657, 5.0078, and 6.3066, respectively for the SFS-NN-MLP, EHO–NN–MLP, and SMA–NN–MLP, all models achieved a satisfactory prediction. This statement can be supported by the PPCCs of 78.06 %, 73.95 %, and 58.11 %.

Fig. 5(a–c) demonstrate the testing results. Similar to the training phase, these figures indicate a suitable testing performance for all three models, whereas the SFS-NN-MLP and EHO–NN–MLP performed more promisingly than SMA–NN–MLP.

3.4. Importance analysis

Feature analysis is a popular type of statistical analysis in machine learning models [80]. A statistical technique, namely principal component analysis (PCA) [81] is employed in this section to investigate the applied dataset in terms of factor importance. As is known, the PCA is based on creating a set of independent components and evaluating their eigenvalues (with 1 as the threshold). Referring to the results in Fig. 6, four components are characterized with eigenvalues greater than 1 which according to statistical reports, they are responsible for 83.61 % variation in the dataset. Therefore, these four components are selected for further analysis.

The selected components are then subjected to a well-known rotation method, namely Varimax with Kaiser Normalization, to achieve Table 2. In this table, the loading factor (LF) attributing to the input factors of each component are presented. Based on the defined thresholds $|LF| > 0.75$, the most important inputs can be detected. The importance of IF_4 and IF_6 can be seen from Component 1, IF_2 can be seen from Component 2, IF_1 and IF_3 can be seen from Component 3, and IF_7 can be seen from Component 4. Hence, IF_5 is the only IF without significant importance.

These results suggest the idea of eliminating the effect of water content from the used dataset and investigating the changes caused. Although possible accuracy improvement needs running the models with the reduced dataset and checking the evaluation criteria, the

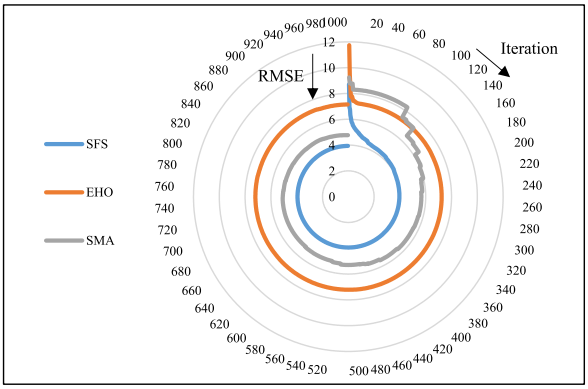

Fig. 3. Radar diagram of the convergence of the SFS, EHO, and SMA optimization.

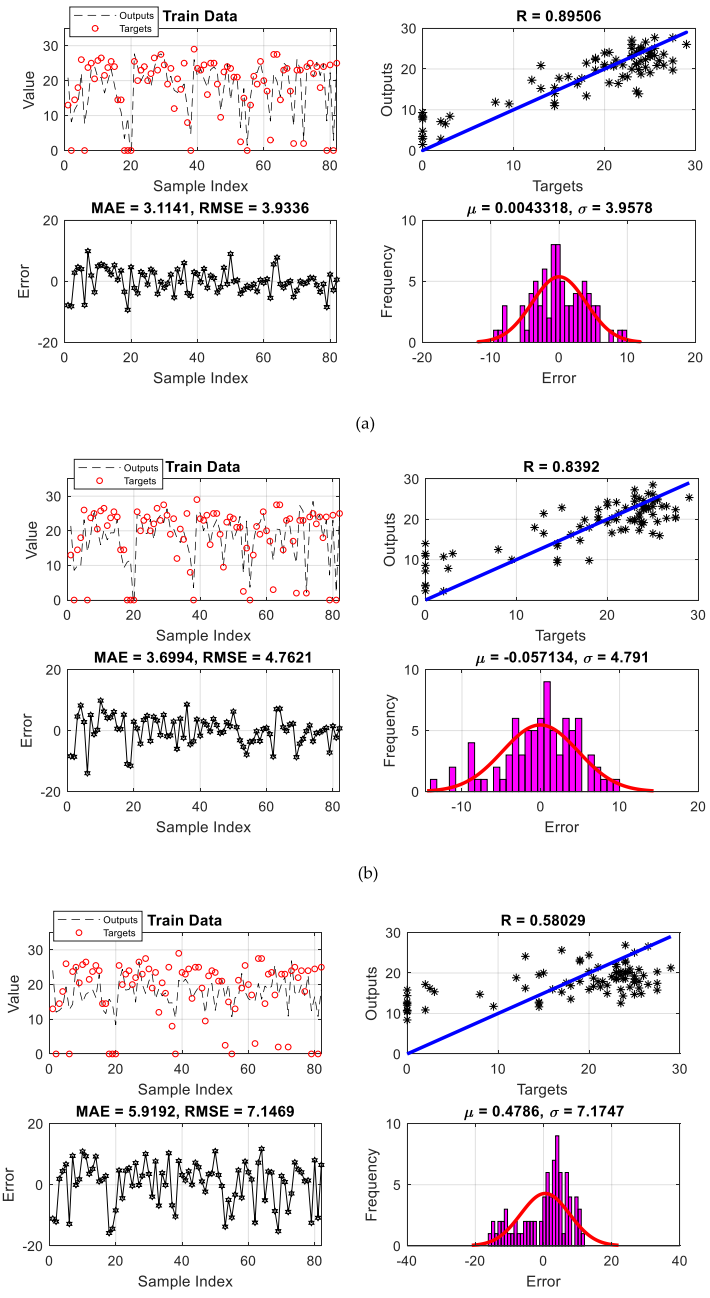

Fig. 4. Correlation and error diagrams of the training operation corresponding to (a) SFS, (b) SMA, and (c) EHO algorithms.

new dataset certainly has a lower dimension that results in more efficient calculations.

3.5. Discussion

The world of science has witnessed many developments and evaluative advances in various domains [82]. One of these advances is ML which has shown great promise in predicting engineering parameters [83,84]. Concrete is one of the most popular materials that has been used for producing structural elements [85–88]. Many studies have proven the applicability of ML in analyzing the mechanical parameters of this material. In this work, three metaheuristic-based NN-MLPs were applied to the prediction of slump, as a crucial concrete parameter.

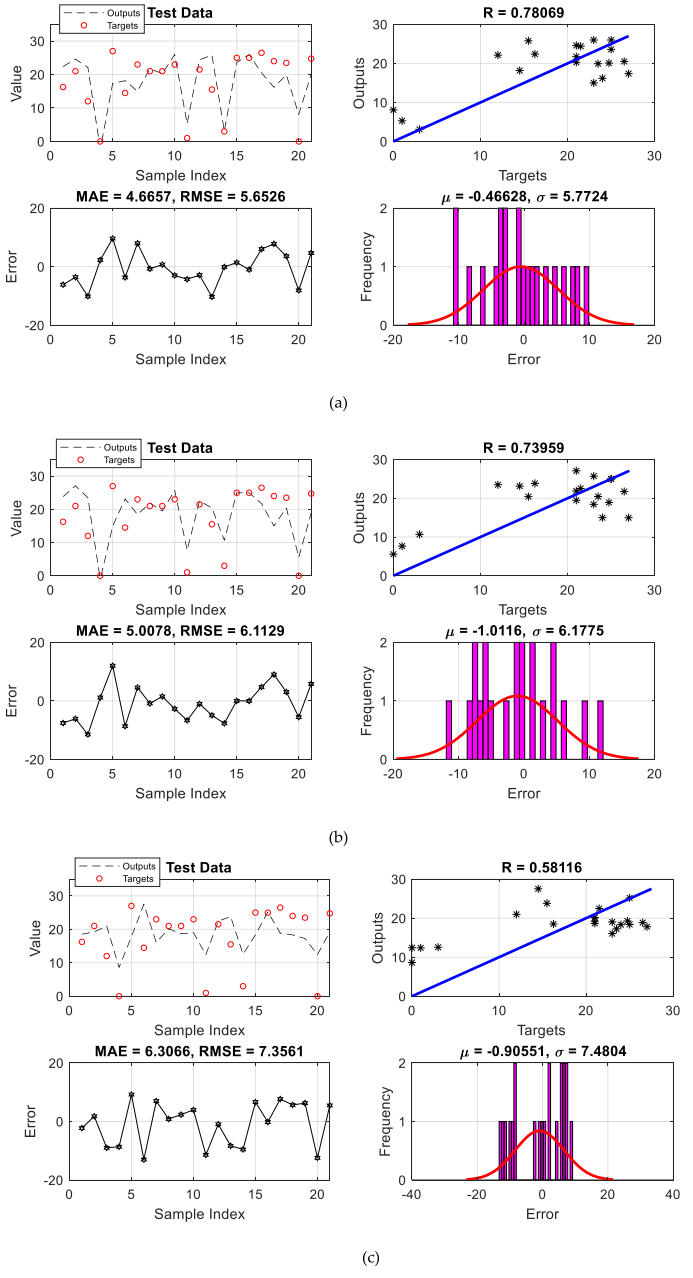

Fig. 5. Correlation and error diagrams of the testing operation corresponding to (a) SFS, (b) SMA, and (c) EHO algorithms.

According to the results, the models achieved satisfying accuracy in both training and testing stages. Employing metaheuristic algorithms provides a secured training for the predictive helping its solution to avoid issues such as overfitting. The range of the predicted and observed slump values in Figs. 4 and 5 supports this claim for the case of this study. Furthermore, Fig. 3 showed that the used metaheuristic algorithms had desirable convergence; providing desirable weights and biases for slump modeling by NN-MLP.

The models showed different levels of accuracy which call for a thorough comparison among them. Supplementary Material (S1) provides the detailed values of $S_{i\ pred}$ and $S_{i\ obs}$. A comparison showed that SMA–NN–MLP could not compete with SFS-NN-MLP and EHO–NN–MLP closely. Also, between the two superior models, the SFS-NN-MLP achieved higher correlation and lower errors at the same time. These claims can be supported by the calculated a20-indices of 0.6712, 0.6575, and 0.3973 for the training results and 0.4737, 0.3684, and 0.3158 for the training results of the SFS-NN-MLP, EHO–NN–MLP, and SMA–NN–MLP, respectively. Therefore, it can be concluded that the SFS-NN-MLP is the most accurate predictive model of this study for slump prediction, followed by the EHO–NN–MLP and SMA–NN–MLP. Besides, from a computational point of view, although the skeleton of all models was an NN-MLP with $7 \times 7 \times 1$ configuration (i.e., seven input neurons, seven hidden neurons, and one output neuron), there were some distinctions

Fig. 6. Results of PCA in terms of eigenvalues.

Table 2
Acquired loading factors of each component (Bold indicates significant values).

	Component			
	1	2	3	4
Slag (IF_1)	0.146	−0.284	**0.863**	0.034
Fly ash (IF_2)	0.207	**0.864**	0.000	−0.300
Superplasticizer (IF_3)	−0.113	−0.349	**−0.835**	−0.106
Coarse aggregate (IF_4)	**0.892**	−0.123	0.150	−0.030
Water (IF_5)	−0.214	0.726	0.013	0.296
Fine aggregate (IF_6)	**−0.813**	−0.176	−0.117	−0.415
Cement (IF_7)	0.175	−0.022	0.093	**0.932**

between the population of optimization algorithms. In this sense, the SFS and SMA algorithms were implemented with the population size = 400, while this parameter was 200 for the EHO.

As with any scientific effort, there were some challenges/limitations in conducting this research. For example, when it comes to hybrid MLs, proper selection of hyperparameters (e.g., the number of hidden neurons, population size, etc.) is important and challenging [54,55]. In this work, this task was tackled by referring to (i) the previous applications of the models to see what are key hyperparameters, (ii) the experts' and authors' experience, and (iii) conducting extensive sensitivity analysis. A notable limitation of this study was the lack of public sources to expand the used dataset [62] (see Section 2.1). Knowing that using a more comprehensive dataset results in a richer training of the models, a potential research avenue for future studies is enriching the data to deal with different concrete mixtures, environmental conditions, and testing scenarios. Apart from data enrichment, feature selection methods (e.g., the used PCA) can be applied toward dimension reduction. Last but not least, the outstanding model of this research (i.e., the SFS-NN-MLP) can be compared to other hybrid tools with two perspectives (i) replacing the SFS with newest optimizers (e.g., walrus optimization algorithm [89], one-to-one-based optimizer [90], gold rush optimizer [91], etc.): and (ii) replacing the NN-MLP with other predictors (e.g., ANFIS [92] and random forest [93]).

4. Conclusions

Slump is a pivotal factor that reflects the quality of the concrete mixture. This research was a structural-computational effort to provide reliable solutions to the early analysis of concrete slump. The suggested solutions were acquired by hybrid machine learning models that comprised a multi-layer perceptron neural network (NN-MLP) coupled with stochastic fractal search (SFS), elephant herding optimization algorithm (EHO), and slime mould algorithm (SMA). These three models analyzed the dependency of the slump on seven concrete ingredients and achieved a reliable understanding. In the subsequent phase, their knowledge was assessed by predicting the slump of 21 unseen specimens. Based on the accuracy assessment, all three models performed satisfactorily, however, the higher accuracy of the SFS-NN-MLP was evident. Therefore, this model was introduced as an outcome of this study. Additionally, a statistical importance assessment was performed on the dataset which revealed the critical importance of almost all input factors in the slump prediction. In future research attempts, experts are recommended to focus on improving the solutions in hand by focusing on the use of external datasets, as well as double-metaheuristic algorithms for training the NN-MLP.

Funding

This work was supported by Jiangxi Provincial Natural Science Foundation (20232BAB214069).

Data availability

The data analyzed during this study is taken from a public source (UC Irvine Machine Learning Repository: http://archive.ics.uci.edu/dataset/182/concrete+slump+test) based on a study by Yeh [62].

CRediT authorship contribution statement

Yunwen Zhou: Investigation. **Zhihai Jiang:** Investigation. **Xizhen Zhu:** Investigation.

Declaration of competing interest

The authors declare that they have no known competing financial interests or personal relationships that could have appeared to influence the work reported in this paper.

Appendix A. Supplementary data

Supplementary data to this article can be found online at https://doi.org/10.1016/j.heliyon.2024.e30677.

References

[1] M. Wang, X. Yang, W. Wang, Establishing a 3D aggregates database from X-ray CT scans of bulk concrete, Construct. Build. Mater. 315 (2022) 125740.
[2] Y. Tang, Y. Wang, D. Wu, M. Chen, L. Pang, J. Sun, W. Feng, X. Wang, Exploring temperature-resilient recycled aggregate concrete with waste rubber: an experimental and multi-objective optimization analysis, Rev. Adv. Mater. Sci. 62 (1) (2023) 20230347.
[3] C. Zhou, J. Wang, X. Shao, L. Li, J. Sun, X. Wang, The feasibility of using ultra-high performance concrete (UHPC) to strengthen RC beams in torsion, J. Mater. Res. Technol. 24 (2023) 9961–9983.
[4] W. Zhang, S. Kang, B. Lin, Y. Huang, Mixed-mode debonding in CFRP-to-steel fiber–reinforced concrete joints, J. Compos. Construct. 28 (1) (2024) 04023069.
[5] X. Zhang, S. Wang, H. Liu, J. Cui, C. Liu, X. Meng, Assessing the impact of inertial load on the buckling behavior of piles with large slenderness ratios in liquefiable deposits, Soil Dynam. Earthq. Eng. 176 (2024) 108322.
[6] A.K. Al-Shamiri, T.-F. Yuan, Non-Tuned machine learning approach for predicting the compressive strength of high-performance concrete, Materials 13 (5) (2020) 1023.
[7] M.R. Goriparthi, G.R. Td, Effect of fly ash and GGBS combination on mechanical and durability properties of GPC, Advances in Concrete Construction 5 (4) (2017) 313.
[8] S. Saha, C. Rajasekaran, Mechanical properties of recycled aggregate concrete produced with Portland Pozzolana Cement, Advances in Concrete Construction 4 (1) (2016) 27.
[9] A. Bakhshi, R. Sedghi, M. Hojati, A preliminary study on the mix design of 3D-printable engineered cementitious composite, in: Tran-SET 2021, American Society of Civil Engineers Reston, VA, 2021, pp. 199–211.
[10] N. Shakouri Mahmoudabadi, A. Bahrami, S. Saghir, A. Ahmad, M. Iqbal, M. Elchalakani, Y.O. Özkılıç, Effects of eccentric loading on performance of concrete columns reinforced with glass fiber-reinforced polymer bars, Sci. Rep. 14 (1) (2024) 1890.
[11] M. Mozafarjazia, R. Rabieeb, Experimental and numerical study on the load-bearing capacity, ductility and energy absorption of RC shear walls with opening containing zeolite and silica fume, Engineering Solid Mechanics (2024).
[12] J. Cao, S.-T. Quek, H. Xiong, Z. Yang, Comparison of constrained unscented and cubature Kalman filters for nonlinear system parameter identification, J. Eng. Mech. 149 (11) (2023) 04023088.
[13] C. Liu, J. Cui, Z. Zhang, H. Liu, X. Huang, C. Zhang, The role of TBM asymmetric tail-grouting on surface settlement in coarse-grained soils of urban area: field tests and FEA modelling, Tunn. Undergr. Space Technol. 111 (2021) 103857.
[14] C. Fu, H. Yuan, H. Xu, H. Zhang, L. Shen, TMSO-Net: texture adaptive multi-scale observation for light field image depth estimation, J. Vis. Commun. Image Represent. 90 (2023) 103731.
[15] C. Ren, J. Yu, C. Zhang, X. Liu, Y. Zhu, W. Yao, Micro–macro approach of anisotropic damage: a semi-analytical constitutive model of porous cracked rock, Eng. Fract. Mech. 290 (2023) 109483.
[16] Z. Chen, L. Chen, X. Zhou, L. Huang, M. Sandanayake, P.-S. Yap, Recent technological advancements in BIM and LCA integration for sustainable construction: a review, Sustainability 16 (3) (2024) 1340.
[17] J. Cao, F. Bu, J. Wang, C. Bao, W. Chen, K. Dai, Reconstruction of full-field dynamic responses for large-scale structures using optimal sensor placement, J. Sound Vib. 554 (2023) 117693.
[18] B. Pang, H. Zheng, Z. Jin, D. Hou, Y. Zhang, X. Song, Y. Sun, Z. Liu, W. She, L. Yang, Inner superhydrophobic materials based on waste fly ash: microstructural morphology of microetching effects, Compos. B Eng. 268 (2024) 111089.
[19] H. Huang, M. Li, W. Zhang, Y. Yuan, Seismic behavior of a friction-type artificial plastic hinge for the precast beam–column connection, Arch. Civ. Mech. Eng. 22 (4) (2022) 201.
[20] H. He, J. Shi, S. Yu, J. Yang, K. Xu, C. He, X. Li, Exploring green and efficient zero-dimensional carbon-based inhibitors for carbon steel: from performance to mechanism, Construct. Build. Mater. 411 (2024) 134334.
[21] L. Sun, T. Liang, C. Zhang, J. Chen, The rheological performance of shear-thickening fluids based on carbon fiber and silica nanocomposite, Phys. Fluids 35 (3) (2023).
[22] W. Liu, J. Liang, T. Xu, Tunnelling-induced ground deformation subjected to the behavior of tail grouting materials, Tunn. Undergr. Space Technol. 140 (2023) 105253.
[23] C. Ren, J. Yu, X. Liu, Z. Zhang, Y. Cai, Cyclic constitutive equations of rock with coupled damage induced by compaction and cracking, Int. J. Min. Sci. Technol. 32 (5) (2022) 1153–1165.

[24] L. Chen, Y. Zhang, Z. Chen, Y. Dong, Y. Jiang, J. Hua, Y. Liu, A.I. Osman, M. Farghali, L. Huang, Biomaterials technology and policies in the building sector: a review, Environ. Chem. Lett. (2024) 1–36.
[25] M.-L. Shi, L. Lv, L. Xu, A multi-fidelity surrogate model based on extreme support vector regression: fusing different fidelity data for engineering design, Eng. Comput. 40 (2) (2023) 473–493.
[26] X. Yao, X. Lyu, J. Sun, B. Wang, Y. Wang, M. Yang, Y. Wei, M. Elchalakani, D. Li, X. Wang, AI-based performance prediction for 3D-printed concrete considering anisotropy and steam curing condition, Construct. Build. Mater. 375 (2023) 130898.
[27] H. Yin, Q. Wu, S. Yin, S. Dong, Z. Dai, M.R. Soltanian, Predicting mine water inrush accidents based on water level anomalies of borehole groups using long short-term memory and isolation forest, J. Hydrol. 616 (2023) 128813.
[28] P.G. Asteris, A.D. Skentou, A. Bardhan, P. Samui, P.B. Lourenço, Soft computing techniques for the prediction of concrete compressive strength using Non-Destructive tests, Construct. Build. Mater. 303 (2021) 124450.
[29] A. Ghasemi, M. Naser, in: *Tailoring 3D Printed Concrete through Explainable Artificial Intelligence*, Structures, Elsevier, 2023 104850, 2023.
[30] A. Kumar, H.C. Arora, N.R. Kapoor, M.A. Mohammed, K. Kumar, A. Majumdar, O. Thinnukool, Compressive strength prediction of lightweight concrete: machine learning models, Sustainability 14 (4) (2022) 2404.
[31] B.A. Salami, T. Olayiwola, T.A. Oyehan, I.A. Raji, Data-driven model for ternary-blend concrete compressive strength prediction using machine learning approach, Construct. Build. Mater. 301 (2021) 124152.
[32] Y. Zhao, H. Hu, C. Song, Z. Wang, Predicting compressive strength of manufactured-sand concrete using conventional and metaheuristic-tuned artificial neural network, Measurement 194 (2022) 110993.
[33] X. Long, M.-h. Mao, T.-x. Su, Y.-t. Su, M.-k. Tian, Machine learning method to predict dynamic compressive response of concrete-like material at high strain rates, Defence Technology 23 (2023) 100–111.
[34] G. Jiang, J. Keller, P.L. Bond, Z. Yuan, Predicting concrete corrosion of sewers using artificial neural network, Water Res. 92 (2016) 52–60.
[35] R. Parichatprecha, P. Nimityongskul, Analysis of durability of high performance concrete using artificial neural networks, Construct. Build. Mater. 23 (2) (2009) 910–917.
[36] F. Demir, Prediction of elastic modulus of normal and high strength concrete by artificial neural networks, Construct. Build. Mater. 22 (7) (2008) 1428–1435.
[37] C.H. Nguyen, L.H. Tran, K.N. Ho, Application of neural network to predict the workability parameters of self-compacting concrete, in: CIGOS 2019, Innovation for Sustainable Infrastructure, Springer, 2020, pp. 1161–1166.
[38] A. Hammoudi, K. Moussaceb, C. Belebchouche, F. Dahmoune, Comparison of artificial neural network (ANN) and response surface methodology (RSM) prediction in compressive strength of recycled concrete aggregates, Construct. Build. Mater. 209 (2019) 425–436.
[39] A.T. Amlashi, S.M. Abdollahi, S. Goodarzi, A.R. Ghanizadeh, Soft computing based formulations for slump, compressive strength, and elastic modulus of bentonite plastic concrete, J. Clean. Prod. 230 (2019) 1197–1216.
[40] O. Onikeku, S.M. Shitote, J. Mwero, A. Adedeji, C. Kanali, Compressive strength and slump prediction of two blended agro waste materials concretes, Open Civ. Eng. J. 13 (1) (2019).
[41] N.-D. Hoang, A.-D. Pham, Estimating concrete workability based on slump test with least squares support vector regression, Journal of construction engineering 2016 (2016).
[42] M.A. DeRousseau, J.R. Kasprzyk, W.V. Srubar, Computational design optimization of concrete mixtures: a review, Cement Concr. Res. 109 (2018) 42–53.
[43] A. Behnood, V. Behnood, M. Modiri Gharehveran, K.E. Alyamac, Prediction of the compressive strength of normal and high-performance concretes using M5P model tree algorithm, Construct. Build. Mater. 142 (2017) 199–207.
[44] M. Mosavi, M. Khishe, A. Moridi, Classification of sonar target using hybrid particle swarm and gravitational search, Iranian journal of Marine technology 3 (1) (2021) 1–13.
[45] F. Chen, C. Yang, M. Khishe, Diagnose Parkinson's disease and cleft lip and palate using deep convolutional neural networks evolved by IP-based chimp optimization algorithm, Biomed. Signal Process Control 77 (2022) 103688.
[46] A. Saffari, M. Khishe, Classification of Marine Mammals Using Trained Multilayer Perceptron Neural Network with Whale Algorithm Developed with Fuzzy System, 2020.
[47] S. Wahab, M. Suleiman, F. Shabbir, N.S. Mahmoudabadi, S. Waqas, N. Herl, A. Ahmad, Predicting confinement effect of carbon fiber reinforced polymers on strength of concrete using metaheuristics-based artificial neural networks, Journal of Civil Engineering Frontiers 4 (2) (2023) 45–59.
[48] H. Moayedi, B. Kalantar, L.K. Foong, D. Tien Bui, A. Motevalli, Application of three metaheuristic techniques in simulation of concrete slump, Appl. Sci. 9 (20) (2019) 4340.
[49] V. Chandwani, V. Agrawal, R. Nagar, Modeling slump of ready mix concrete using genetic algorithms assisted training of Artificial Neural Networks, Expert Syst. Appl. 42 (2) (2015) 885–893.
[50] L.K. Foong, Y. Zhao, C. Bai, C. Xu, Efficient metaheuristic-retrofitted techniques for concrete slump simulation, Smart Structures and Systems, An International Journal 27 (5) (2021) 745–759.
[51] J. Zhang, Y. Huang, Y. Wang, G. Ma, Multi-objective optimization of concrete mixture proportions using machine learning and metaheuristic algorithms, Construct. Build. Mater. 253 (2020) 119208.
[52] J. Zhang, Y. Huang, G. Ma, B. Nener, Mixture optimization for environmental, economical and mechanical objectives in silica fume concrete: a novel frame-work based on machine learning and a new meta-heuristic algorithm, Resour. Conserv. Recycl. 167 (2021) 105395.
[53] H.-B. Ly, M.H. Nguyen, B.T. Pham, Metaheuristic optimization of Levenberg–Marquardt-based artificial neural network using particle swarm optimization for prediction of foamed concrete compressive strength, Neural Comput. Appl. 33 (24) (2021) 17331–17351.
[54] H. Safayenikoo, F. Nejati, M.L.J.S. Nehdi, Indirect analysis of concrete slump using different metaheuristic-empowered neural processors 14 (16) (2022) 10373.
[55] H. Safayenikoo, M. Khajehzadeh, M.L. Nehdi, Novel Evolutionary-Optimized Neural Network for Predicting Fresh Concrete Slump. 14 (9) (2022) 4934.
[56] H. Salimi, Stochastic fractal search: a powerful metaheuristic algorithm, Knowl. Base Syst. 75 (2015) 1–18.
[57] J. Ye, J. Dalle, R. Nezami, M. Hasanipanah, D.J. Armaghani, Stochastic fractal search-tuned ANFIS model to predict blast-induced air overpressure, Eng. Comput. (2022) 1–15.
[58] H. Moayedi, A.A. Dehrashid, M.H. Gholizadeh, A novel hybrid based on nature-inspired and Stochastic Fractal Search algorithms for optimizing of artificial neural network model in landslide susceptibility, Eng. Appl. Artif. Intell. 117 (2023) 105457.
[59] F. Nejati, W.O. Zoy, N. Tahoori, P. Abdunabi Xalikovich, M.A. Sharifian, M.L. Nehdi, Machine learning method based on symbiotic organism search algorithm for thermal load prediction in buildings, Buildings 13 (3) (2023) 727.
[60] G.-G. Wang, S. Deb, L.d.S. Coelho, in: *Elephant Herding Optimization*, 2015 3rd International Symposium on Computational and Business Intelligence (ISCBI), 2015, IEEE, 2015, pp. 1–5.
[61] S. Li, H. Chen, M. Wang, A.A. Heidari, S. Mirjalili, Slime mould algorithm: a new method for stochastic optimization, Future Generat. Comput. Syst. (2020).
[62] I.-C. Yeh, Modeling slump flow of concrete using second-order regressions and artificial neural networks, Cement Concr. Compos. 29 (6) (2007) 474–480.
[63] M.A. El-Hameed, M.M. Elkholy, A.A. El-Fergany, Efficient frequency regulation in highly penetrated power systems by renewable energy sources using stochastic fractal optimiser, IET Renew. Power Gener. 13 (12) (2019) 2174–2183.
[64] M. Khishe, M. Mosavi, A. Moridi, Chaotic fractal walk trainer for sonar data set classification using multi-layer perceptron neural network and its hardware implementation, Appl. Acoust. 137 (2018) 121–139.
[65] M.R. Mosavi, M. Khishe, Y. Hatam Khani, M. Shabani, Training radial basis function neural network using stochastic fractal search algorithm to classify sonar dataset, Iran J Electr Electron Eng 13 (1) (2017) 100–111.
[66] H. Mosbah, M. El-Hawary, Optimization of neural network parameters by Stochastic Fractal Search for dynamic state estimation under communication failure, Elec. Power Syst. Res. 147 (2017) 288–301.
[67] H.A. Akar, F.R. Mahdi, Research article trajectory tracking controller of mobile robot under time variation parameters based on neural networks and stochastic fractal algorithm, Res. J. Appl. Sci. Eng. Technol. 13 (11) (2016) 871–878.

[68] P.K. Rawlings, Modes of a Gaussian random walk, J. Stat. Phys. 111 (3–4) (2003) 769–788.
[69] R. Sukumar, The Asian Elephant: Ecology and Management, Cambridge University Press, 1992.
[70] R. Vijay, Optimal allocation of electric power distributed generation on distributed network using elephant herding optimization technique, CVR Journal of Science and Technology 15 (2018) 73–79.
[71] T. Latty, M. Beekman, Food quality and the risk of light exposure affect patch-choice decisions in the slime mold Physarum polycephalum, Ecology 91 (1) (2010) 22–27.
[72] P.G. Asteris, M. Koopialipoor, D.J. Armaghani, E.A. Kotsonis, P.B. Lourenço, Prediction of cement-based mortars compressive strength using machine learning techniques, Neural Comput. Appl. 33 (19) (2021) 13089–13121.
[73] D. Sun, M. Lonbani, B. Askarian, D. Jahed Armaghani, R. Tarinejad, B. Thai Pham, V.V. Huynh, Investigating the applications of machine learning techniques to predict the rock brittleness index, Appl. Sci. 10 (5) (2020) 1691.
[74] S. Paudel, A. Pudasaini, R.K. Shrestha, E. Kharel, Compressive strength of concrete material using machine learning techniques, Cleaner Engineering and Technology 15 (2023) 100661.
[75] H. Chen, P.G. Asteris, D. Jahed Armaghani, B. Gordan, B.T. Pham, Assessing dynamic conditions of the retaining wall: developing two hybrid intelligent models, Appl. Sci. 9 (6) (2019) 1042.
[76] P.G. Asteris, S. Nozhati, M. Nikoo, L. Cavaleri, M. Nikoo, Krill herd algorithm-based neural network in structural seismic reliability evaluation, Mech. Adv. Mater. Struct. 26 (13) (2019) 1146–1153.
[77] Y. Wang, L. Yuan, M. Khishe, A. Moridi, F. Mohammadzade, Training RBF NN using sine-cosine algorithm for sonar target classification, Arch. Acoust. Q. 45 (4) (2020) 753–764.
[78] S. Mousavi, M. Kaveh, M. Khishe, Sonar data set classification using MLP neural network trained by modified biogeography-based optimization, Iranian Journal of Marine Science and Technology 20 (78) (2016) 65–74.
[79] M. Mosavi, M. Kaveh, M. Khishe, M. Aghababaee, Design and implementation a sonar data set classifier by using MLP NN trained by improved biogeography-based optimization, Proceedings of the Second National Conference on marine technology 2016 (2016) 1–6.
[80] H. Kosarirad, M. Ghasempour Nejati, A. Saffari, M. Khishe, M. Mohammadi, Feature selection and training multilayer perceptron neural networks using grasshopper optimization algorithm for design optimal classifier of big data sonar, J. Sens. 2022 (2022).
[81] H. Abdi, L.J. Williams, Principal component analysis, Wiley Interdiscip. Rev. Comput. Stat. 2 (4) (2010) 433–459.
[82] P.X. McCarthy, X. Gong, S. Eghbal, D.S. Falster, M.-A. Rizoiu, Evolution of diversity and dominance of companies in online activity, PLoS One 16 (4) (2021) e0249993.
[83] M. Hajihassani, S.S. Abdullah, P.G. Asteris, D.J. Armaghani, A gene expression programming model for predicting tunnel convergence, Appl. Sci. 9 (21) (2019) 4650.
[84] P.G. Asteris, A.K. Tsaris, L. Cavaleri, C.C. Repapis, A. Papalou, F. Di Trapani, D.F. Karypidis, Prediction of the fundamental period of infilled RC frame structures using artificial neural networks, Comput. Intell. Neurosci. 2016 (2016), 20-20.
[85] H. Huang, Y. Yuan, W. Zhang, L. Zhu, Property assessment of high-performance concrete containing three types of fibers, International Journal of Concrete Structures and Materials 15 (1) (2021) 1–17.
[86] H. Huang, M. Guo, W. Zhang, M. Huang, Seismic behavior of strengthened RC columns under combined loadings, J. Bridge Eng. 27 (6) (2022) 05022005.
[87] L. Sun, C. Wang, C. Zhang, Z. Yang, C. Li, P. Qiao, Experimental investigation on the bond performance of sea sand coral concrete with FRP bar reinforcement for marine environments, Adv. Struct. Eng. 26 (3) (2023) 533–546.
[88] X. Wang, L. Li, Y. Xiang, Y. Wu, M. Wei, The influence of basalt fiber on the mechanical performance of concrete-filled steel tube short columns under axial compression, Frontiers in Materials 10 (2024) 1332269.
[89] P. Trojovský, M. Dehghani, A new bio-inspired metaheuristic algorithm for solving optimization problems based on walruses behavior, Sci. Rep. 13 (1) (2023) 8775.
[90] M. Dehghani, E. Trojovská, P. Trojovský, O.P. Malik, OOBO: a new metaheuristic algorithm for solving optimization problems, Biomimetics 8 (6) (2023) 468.
[91] K. Zolf, Gold rush optimizer: a new population-based metaheuristic algorithm, Operations Research and Decisions 33 (1) (2023).
[92] J.-S. Jang, ANFIS: adaptive-network-based fuzzy inference system, IEEE transactions on systems, man, and cybernetics 23 (3) (1993) 665–685.
[93] L. Breiman, Bagging predictors, Mach. Learn. 24 (2) (1996) 123–140.